Journal of Solid State Chemistry 184 (2011) 2278–2284

Contents lists available at ScienceDirect

Journal of Solid State Chemistry

journal homepage: www.elsevier.com/locate/jssc

Synthesis and structural characterization of $Al_7C_3N_3$-homeotypic aluminum silicon oxycarbonitride, $(Al_{7-x}Si_x)(O_yC_zN_{6-y-z})$ ($x\sim1.2$, $y\sim1.0$ and $z\sim3.5$)

Daisuke Urushihara [a], Motoaki Kaga [a], Toru Asaka [a], Hiromi Nakano [b], Koichiro Fukuda [a,*]

[a] Department of Environmental and Materials Engineering, Nagoya Institute of Technology, Nagoya 466-8555, Japan
[b] Cooperative Research Facility Center, Toyohashi University of Technology, Toyohashi 441-8580, Japan

ARTICLE INFO

Article history:
Received 3 May 2011
Received in revised form
23 June 2011
Accepted 24 June 2011
Available online 1 July 2011

Keywords:
Aluminum silicon oxycarbonitrides
Crystal structures
Rietveld method
Domain structures
$Al_7C_3N_3$
$Al_8C_3N_4$

ABSTRACT

A new aluminum silicon oxycarbonitride, $(Al_{5.8}Si_{1.2})(O_{1.0}C_{3.5}N_{1.5})$, has been synthesized and characterized by X-ray powder diffraction (XRPD), transmission electron microscopy (TEM), energy dispersive X-ray spectroscopy (EDX) and electron energy loss spectroscopy (EELS). The title compound is hexagonal with space group $P6_3/mmc$ and unit-cell dimensions $a=0.322508(4)$ nm, $c=3.17193(4)$ nm and $V=0.285717(6)$ nm^3. The atom ratios of Al:Si and those of O:C:N were, respectively, determined by EDX and EELS. The initial structural model was successfully derived from the XRPD data by the direct methods and further refined by the Rietveld method. The crystal is most probably composed of four types of domains with nearly the same fraction, each of which is isotypic to $Al_7C_3N_3$ with space group $P6_3mc$. The existence of another new oxycarbonitride $(Al_{6.6}Si_{1.4})(O_{0.7}C_{4.3}N_{2.0})$, which must be homeotypic to $Al_8C_3N_4$, has been also demonstrated by XRPD and TEM.

1. Introduction

Carbonitrides, oxycarbides and oxycarbonitrides have attracted significant attention because of their wide potential applicability in phosphors, refractories and fibers for reinforced composite materials [1–3]. A series of ternary carbonitrides in the Al_4C_3–AlN system [4,5] can be represented by a general formula $Al_4C_3(AlN)_X$, where $X=1$ (Al_5C_3N), 2 ($Al_6C_3N_2$), 3 ($Al_7C_3N_3$) and 4 ($A1_8C_3N_4$). These carbonitrides have the characteristics of layered structures consisting of two types of layers. One is an $[Al_4(C, N)_4]$ unit layer (A), which is composed of an $[Al_2(C, N)_2]$ double layer of Al(C, N)$_4$ tetrahedra surrounded by two $[Al(C, N)_2]$ single layers of Al(C, N)$_4$ tetrahedra. The other is an $[Al(C, N)_2]$ single layer (B) of Al(C, N)$_4$ tetrahedra. The structure of $Al_7C_3N_3$ (space group $P6_3mc$, $Z=2$) is build up of alternately stacking two types of layers with the sequence of $\langle BBABBBAB\rangle$ (Fig. 1a). For the rhombohedral lattice of $A1_8C_3N_4$ ($R\bar{3}m$ or $R3m$, $Z=3$), the stacking sequence is $\langle BBABBBBABBBBABB\rangle$ (Fig. 1b). The crystal structures of the other aluminum carbonitrides are also made up of the combinations of A and B layers with the stacking sequences of $\langle BABA\rangle$ for Al_5C_3N (space group $P6_3mc$, $Z=2$) and $\langle BABBABBAB\rangle$ for $Al_6C_3N_2$ ($R\bar{3}m$ or $R3m$, $Z=3$).

In the system Al–Si–O–C, the authors have discovered and structurally characterized three types of new aluminum silicon oxycarbides; $(Al_{18-x}Si_x)(O_yC_{14-y})$ ($x\sim1.2$ and $y\sim3.0$) [6], $(Al_{5-x}Si_x)(O_yC_{4-y})$ ($x\sim0.6$ and $y\sim1.0$) [7] and $(Al_{6-x}Si_x)(O_yC_{5-y})$ ($x\sim0.8$ and $y\sim1.6$) [8]. Each of the former two crystals has been found to be made up of two types of domains, which are related by pseudo-symmetry inversion, with the domain ratios being almost 0.5:0.5. The latter crystal has been composed of three types of domains with nearly the same fraction. The dimensions of all these twin domains have been within the coherence range of X-rays, hence the crystal structures have been successfully represented by the split-atom models. Recently, a new aluminum oxycarbonitride $Al_5(O_xC_yN_{4-x-y})$ ($x\sim1.4$ and $y\sim2.1$) [9] has been reported to be isotypic to $(Al_{5-x}Si_x)(O_yC_{4-y})$. All of these compounds in the Al–Si–O–C–N system are build up of A-type [(Al, Si)$_4$(O, C, N)$_4$] unit layer and B-type [(Al, Si)(O, C, N)$_2$] single layer. With $(Al_{4.4}Si_{0.6})(O_{1.0}C_{3.0})$ and $Al_5(O_{1.4}C_{2.1}N_{0.5})$ ($P6_3/mmc$, $Z=2$), the stacking sequences within individual domains are $\langle ABAB\rangle$ and/or $\langle BABA\rangle$, indicating that the atom arrangements of these domains are very similar to those of Al_5C_3N. Thus, $(Al_{4.4}Si_{0.6})(O_{1.0}C_{3.0})$ and $Al_5(O_{1.4}C_{2.1}N_{0.5})$ can be regarded as being homeotypic to Al_5C_3N. The layer stacking sequences are $\langle BABBABBAB\rangle$, $\langle BBABBABBA\rangle$ and/or $\langle ABBABBABB\rangle$ for the three types of domains of $(Al_{5.2}Si_{0.8})(O_{1.6}C_{3.4})$ ($R\bar{3}m$, $Z=3$), which is homeotypic to $Al_6C_3N_2$. In a similar manner, new layered oxycarbonitrides with the chemical formulas (Al, Si)$_7$(O, C, N)$_6$ and (Al, Si)$_8$(O, C, N)$_7$ are expected to form, which can be, respectively, homeotypic to $Al_7C_3N_3$ and $A1_8C_3N_4$. The minimum stacking sequence within the unit cell must be $BBAB$ for (Al, Si)$_7$(O, C, N)$_6$ and $BBABB$ for (Al, Si)$_8$(O, C, N)$_7$. Because the layer thickness of

* Corresponding author. Fax: +81 52 735 5289.
E-mail address: fukuda.koichiro@nitech.ac.jp (K. Fukuda).

0022-4596/$ - see front matter © 2011 Elsevier Inc. All rights reserved.
doi:10.1016/j.jssc.2011.06.030

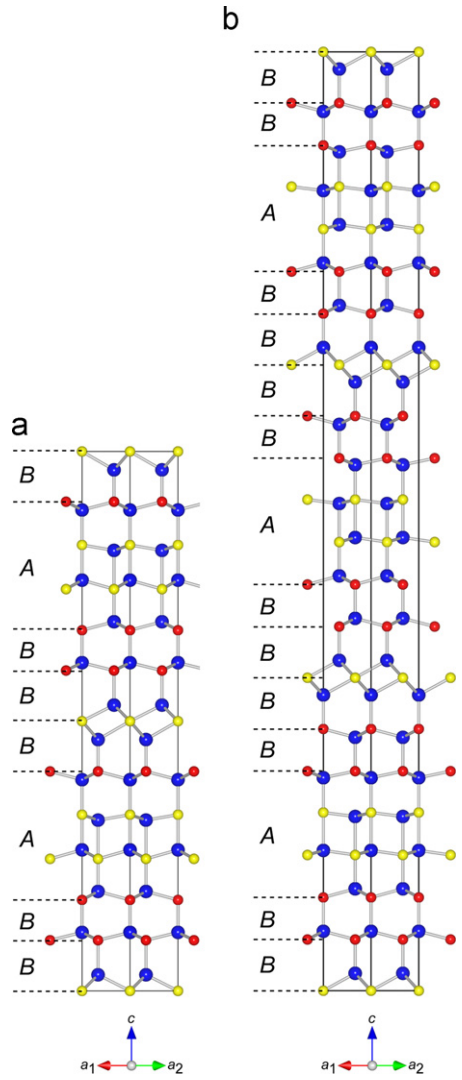

Fig. 1. Atomic configurations in (a) $Al_7C_3N_3$ (space group $P6_3mc$) and (b) $A1_8C_3N_4$ (space group $R3m$), showing the crystal structures being made up of two types of layers *A* and *B*. Blue balls are for aluminum sites, yellow balls are for carbon sites and red balls are for oxygen sites. (For interpretation of the references to color in this figure legend, the reader is referred to the web version of this article.)

A is ~0.75 nm and that of *B* is between 0.24 and 0.30 nm, the expected thickness of *BBAB* ($=d_{002}$) is 1.47–1.65 nm for $(Al, Si)_7(O, C, N)_6$ and that of *BBABB* ($=d_{003}$) is 1.71–1.95 nm for $(Al, Si)_8(O, C, N)_7$.

In the present study, we have succeeded in synthesizing two types of new aluminum silicon oxycarbonitrides, $(Al, Si)_7(O, C, N)_6$ and $(Al, Si)_8(O, C, N)_7$. We determined the initial structural model of the former from XRPD data using direct methods and further modified it into a split-atom model in which two of the four types of Al/Si sites were positionally disordered. The crystal was most probably composed of four types of domains. For the latter aluminum silicon oxycarbonitride, we have revealed the chemical composition and unit-cell dimensions.

2. Experimental

2.1. Synthesis

The two types of new aluminum silicon oxycarbonitrides exhibited the characteristic diffraction peaks at $2\theta \approx 5.57^\circ$ ($d \approx 1.59$ nm) and $2\theta \approx 4.81^\circ$ ($d \approx 1.84$ nm) for Cu$K\alpha_1$ radiation. The corresponding *d*-values strongly suggest that the unknown phases are $(Al, Si)_7(O, C, N)_6$ and $(Al, Si)_8(O, C, N)_7$. We obtained the powder specimen that was mainly consisting of $(Al, Si)_7(O, C, N)_6$ together with small amounts of $(Al, Si)_6(O, C, N)_5$, graphite and $(Al, Si)_8(O, C, N)_7$ by the procedures as described in the following paragraph.

In a previous study, we prepared a powder specimen consisting mainly of $(Al_{5.2}Si_{0.8})(O_{1.6}C_{3.4})$ with a small amount of graphite [8]. In the present study, we used this powder sample as the starting material, which was obtained by the following procedure. The reagent-grade chemicals of Al_4C_3 (98%, Mitsuwa Chemical Co., Ltd., Kanagawa, Japan) and SiC (99%, KCL Co., Ltd., Saitama, Japan) were mixed in molar ratios of Al_4C_3:SiC = 1.5:1. The well-mixed chemicals were pressed into pellets (ϕ15 mm × 10 mm), loaded into an open carbon crucible, heated in a carbon resistance furnace at 2073 K for 1 h in inert gas atmosphere of Ar, followed by cooling to ambient temperature by cutting furnace power. The resulting sample was composed exclusively of $(Al_{4.4}Si_{0.6})(O_{1.0}C_{3.0})$, in accord with a previous study [7]. The slightly sintered material thus obtained was pulverized into fine powder specimen. It was, without pressing into pellets, heated at 2273 K (200 K higher than the preparation temperature of the starting material) for 1 h in inert gas atmosphere of Ar using the same electric furnace, followed by cooling to ambient temperature by cutting furnace power. During the heating process, the thermal oxidation of $(Al_{4.4}Si_{0.6})(O_{1.0}C_{3.0})$ proceeded to obtain the starting material [8].

The starting material thus obtained was pulverized into fine powder specimen. It was, without pressing into pellets, heated at 2273 K for 2 h in inert gas atmosphere of Ar, followed by cooling to ambient temperature by cutting furnace power. During the heating process, the thermal oxidation as well as the thermal nitridation of $(Al_{5.2}Si_{0.8})(O_{1.6}C_{3.4})$ proceeded, the thermodynamics mechanism of which will be discussed afterwards. The resulting slightly sintered material was finely ground to obtain powder specimen.

2.2. Characterization

A diffractometer (X'Pert PRO Alpha-1, PANalytical B.V., Almelo, the Netherlands), equipped with an incident-beam Ge(1 1 1) Johansson monochromator to obtain Cu$K\alpha_1$ radiation and a high-speed detector, was used in the Bragg–Brentano geometry. The X-ray generator was operated at 45 kV and 40 mA. An automatic divergence slit was used to keep a constant illuminated length of 5 mm on the specimen surface. Other experimental conditions were: continuous scan, experimental 2θ range from 3.0044° to 147.9913° (an accuracy in 2θ of $\pm$0.0001°), 8677 total data points and 5.5 h total experimental time. The entire experimental diffraction pattern was employed for the crystal-structure analysis. The structure data were standardized according to rules formulated by Parthé and Gelato [10] using the computer program STRUCTURE TIDY [11]. Structural parameters were refined by the Rietveld method using the computer program RIETAN-FP [12]. The crystal-structure models were visualized with the computer program VESTA [13].

The powder sample was also examined using a transmission electron microscope (TEM; JEM 2100F, JEOL Ltd., Tokyo, Japan) operated at 200 kV and equipped with an energy dispersive X-ray analyzer (EDX; JED-2300, JEOL Ltd., Tokyo, Japan) and an electron energy loss spectrometer (EELS; Enfina, Gatan Inc., Pleasanton, CA, U.S.A.). The powder particles were deposited with ethyl alcohol on a copper grid. Selected area electron diffraction (SAED) patterns and corresponding lattice images were obtained. Chemical analyses were made to quantitatively determine the atom ratios of Al:Si by EDX and those of O:C:N by EELS. The multislice simulation image, which was generated using a software package xHREM™ (HREM Research Inc., Saitama, Japan), was compared with the high resolution image to confirm that the structural model of $A1_8C_3N_4$ is applicable to that of the new material $(Al, Si)_8(O, C, N)_7$.

3. Results and discussion

3.1. TEM characterization of $(Al, Si)_8(O, C, N)_7$

We have examined under TEM a crystal fragment of $(Al, Si)_8(O, C, N)_7$, the chemical composition of which was determined by EDX (Al:Si=0.828:0.172) and EELS (O:C:N=0.10:0.62:0.28) to be $Al_{6.6}Si_{1.4}O_{0.7}C_{4.3}N_{2.0}$. The lattice image (Fig. 2) is characterized by a layered structure with the periodicity of about 5.5 nm (=1.84 nm × 3) along the c axis. The distributions of black and white contrast of the simulated image were qualitatively consistent with those of the corresponding high resolution micrograph, suggesting that the atom arrangements of this material is very similar to those of $Al_8C_3N_4$.

3.2. TEM characterization and structure determination of $(Al, Si)_7(O, C, N)_6$

The SAED pattern in Fig. 3 was successfully indexed with a hexagonal unit cell with dimensions of $a \approx 0.32$ nm and $c \approx 3.2$ nm. The corresponding lattice image strongly suggests that the crystal is characterized by a layered structure with the periodicity of about 3.2 nm (=1.59 nm × 2) along the c axis. The EDX spectrum showed the existence of small amounts of N and O atoms, together with C, Al and Si (Fig. 4). The atom ratios Al:Si were determined for four crystal fragments to be 0.832(9):0.168(9), where the numbers in parentheses indicate standard deviations. The Al:Si ratios were very similar to those of the starting material $(Al_{5.2}Si_{0.8})(O_{1.6}C_{3.4})$ (Al:Si=0.87:0.13). The electron energy loss spectrum showed the existence of O, C and N atoms (Fig. 5). The atom ratios O:C:N were determined for seven crystal fragments to be 0.17(7):0.58(5):0.25(2).

The XRPD pattern also showed the presence of relatively weak diffraction intensities peculiar to $(Al, Si)_6(O, C, N)_5$, graphite and $(Al, Si)_8(O, C, N)_7$. All of the other diffraction peaks belonging to the new material, later identified by $(Al, Si)_7(O, C, N)_6$, were successfully indexed with the hexagonal unit cell. The unit-cell parameters and integrated intensities were refined by the Le Bail method [14], using the computer program RIETAN-FP. The refined cell dimensions were $a=0.322516(4)$ nm and $c=3.17189(4)$ nm. The integrated intensities were examined to check for systematic absence. Systematic absences $l \neq 2n$ for $hh\bar{2}h$ l and $l \neq 2n$ for $000l$ reflections were found, which implies that possible space groups are $P31c$, $P\bar{3}1c$, $P6_3mc$, $P\bar{6}2c$ and $P6_3/mmc$.

Because the atomic scattering factors for Al and Si are almost the same and the oxygen and nitrogen concentrations are relatively low, we used a unit-cell content with [14Al 12C] as input

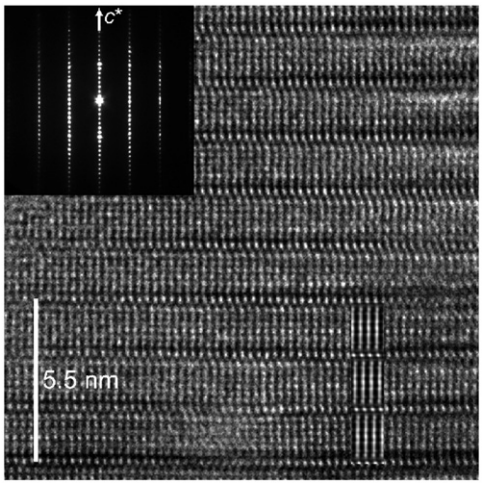

Fig. 2. Selected-area electron diffraction pattern and corresponding lattice image of $(Al_{6.6}Si_{1.4})(O_{0.7}C_{4.3}N_{2.0})$. Incident beam almost parallel to the hexagonal a axis. The simulated image of $A1_8C_3N_4$ (specimen thickness=25.7 nm and defocus value=−390 nm) is inserted in the lattice image.

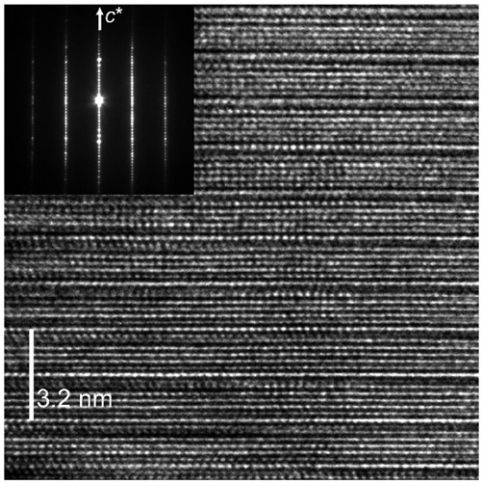

Fig. 3. Selected-area electron diffraction pattern and corresponding lattice image of $(Al_{5.8}Si_{1.2})(O_{1.0}C_{3.5}N_{1.5})$. Incident beam almost parallel to the hexagonal a axis.

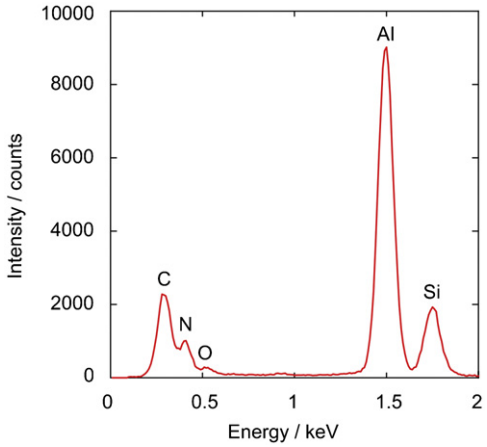

Fig. 4. Identification of the presence of Al, Si, O, C and N in the compound. EDX spectrum.

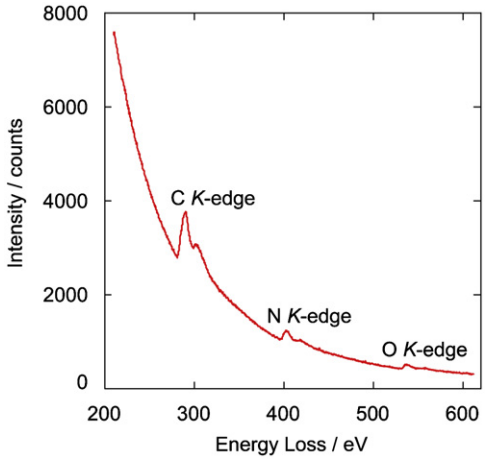

Fig. 5. Identification of the presence of O, C and N in the compound. Electron energy loss spectrum.

data for the search of a crystal-structure model. All of the possible space groups were tested using the EXPO2009 package [15] for crystal structure determination. The individual integrated intensities that were refined by the Le Bail method were used for the direct methods. A promising structural model with a minimum reliability index R_F of 24.3% was found with the space group $P6_3/mmc$ (centrosymmetric). There are eight independent sites in the unit cell; two Al/Si sites (Al/Si3 and Al/Si4) and one O/C/N site (O/C/N4) are located at the Wyckoff position 4*f*, two Al/Si sites (Al/Si1 and Al/Si2) and one O/C/N site (O/C/N3) are located at 4*e*, one O/C/N site (O/C/N1) is located at 2*a* and one O/C/N site (O/C/N2) is located at 2*c*.

3.3. Rietveld analysis

Structural parameters of all atoms were subsequently refined by the Rietveld method [16] using the computer program RIETAN-FP. The structural models of $(Al, Si)_6(O, C, N)_5$ [8], graphite and $(Al, Si)_8(O, C, N)_7$ were included in the refinement as the coexisting phases. The structural parameters of the latter were identical to those of $Al_8C_3N_4$ (space group $R3m$) [5]. A Legendre polynomial was fitted to background intensities with twelve adjustable parameters. The pseudo-Voigt function [17] was used to fit the peak profile. The preferred orientation parameter of March–Dollase function [18] was refined to be 0.873(3) with the preferred-orientation vector [0 0 1], suggesting that the crystal grains were appreciably fractured along the cleavage planes parallel to (0 0 1). The Si and Al atoms were assumed to be randomly distributed over the same sites in the crystal structure, although there might be the site preference of these atoms. The occupancies (g) of O, C and N atoms in each O/C/N site were fixed at $g(O)=0.17$, $g(C)=0.58$ and $g(N)=0.25$, in accordance with the bulk chemical composition. The isotropic displacement (B) parameters of the four O/C/N sites were constrained to be equal. The refinement, however, resulted in the relatively large B parameters for the Al/Si2 and Al/Si4 sites ($B(Al/Si2)=4.5(1)\times10^{-2}$ nm^2 and $B(Al/Si4)=2.15(8)\times10^{-2}$ nm^2) with the less satisfactory reliability (R) indices [19] of $R_{wp}=5.29\%$, S $(=R_{wp}/R_e)=1.71$, $R_p=4.02\%$, $R_B=6.00\%$ and $R_F=3.71\%$. These findings promoted us to build split-atom models for both Al/Si2 and Al/Si4 sites.

In the split-atom model, the Al/Si4 site was split into two independent crystallographic sites, Al/Si4A and Al/Si4B, with the same Wyckoff position 4*f*. The distribution of Al/Si atoms between each of these sites was determined by imposing the linear constrains of $g(Al/Si4A)+g(Al/Si4B)=1$. The parameters $B(Al/Si4A)$ and $B(Al/Si4B)$ were constrained to be equal. On the other hand, the Al/Si2 site was displaced from position 2*b* to position 4*e*, with the point symmetry being reduced from $\bar{6}m2$ to 3*m*. The final Rietveld refinement resulted in satisfactory R indices of $R_{wp}=4.13\%$ ($S=1.34$), $R_p=3.22\%$, $R_B=4.25\%$ and $R_F=2.69\%$, indicating that the disordered arrangements of Al/Si2 and Al/Si4 sites can be represented adequately with the split-atom model in Fig. 6. Observed, calculated, and difference XRPD patterns are plotted in Fig. 7. Crystal data are given in Table 1, and the final atomic positional and B parameters are given in Table 2. The separation distance between the Al/Si4A and Al/Si4B sites was 0.061(1) nm. It should be noted that the g(Al/Si4A)- and g(Al/Si4B)-values converged very close to, respectively, 3/4 and 1/4. The chemical composition was $Al_{5.82(6)}Si_{1.18(6)}O_{1.04(6)}C_{3.5(3)}N_{1.50(9)}$ based on the atom ratios determined by EDX and EELS, with the chemical formula of $(Al_{5.8}Si_{1.2})(O_{1.0}C_{3.5}N_{1.5})$ (space group $P6_3/mmc$, $Z=2$).

Quantitative X-ray analysis with correction for microabsorption according to Brindley's procedure [20] was implemented in the program RIETAN-FP. The phase composition of the sample was found to be 51.7 mass% $(Al_{5.8}Si_{1.2})(O_{1.0}C_{3.5}N_{1.5})$, 30.9 mass% $(Al, Si)_6(O, C, N)_5$, 11.5 mass% $(Al_{6.6}Si_{1.4})(O_{0.7}C_{4.3}N_{2.0})$ and 6.0 mass% graphite, on the assumption that the effective particle radii of these phases were 5.00 mm. The chemical composition of $(Al, Si)_6(O, C, N)_5$ was undetermined in the present study. With $(Al, Si)_8(O, C, N)_7$, the unit-cell dimensions, as given in Table 3 for crystal data, were determined by the Rietveld method, which are in accord with the corresponding SAED pattern (Fig. 2). Further work remains to better understand the exact crystal structure (i.e., structural parameters) as well as the existence of domain structure of $(Al_{6.6}Si_{1.4})(O_{0.7}C_{4.3}N_{2.0})$.

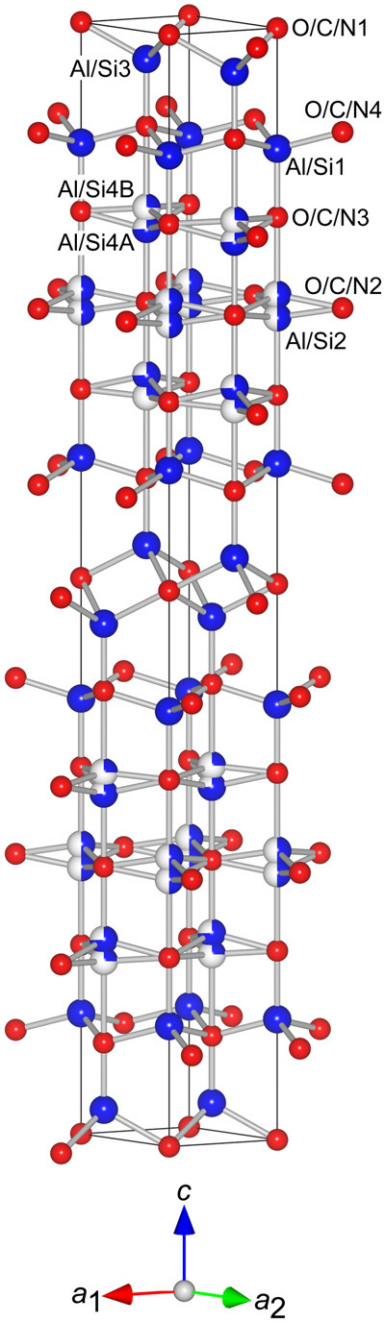

Fig. 6. Crystal structure of $(Al_{5.8}Si_{1.2})(O_{1.0}C_{3.5}N_{1.5})$. Space group $P6_3/mmc$. All the atoms are expressed as solid spheres. Because the occupancies of Al/Si2, Al/Si4A and Al/Si4B sites are less than unity, the Al/Si atoms occupying there are displayed as blue circle graphs for occupancies. Red balls are for oxygen, carbon and nitrogen sites. (For interpretation of the references to color in this figure legend, the reader is referred to the web version of this article.)

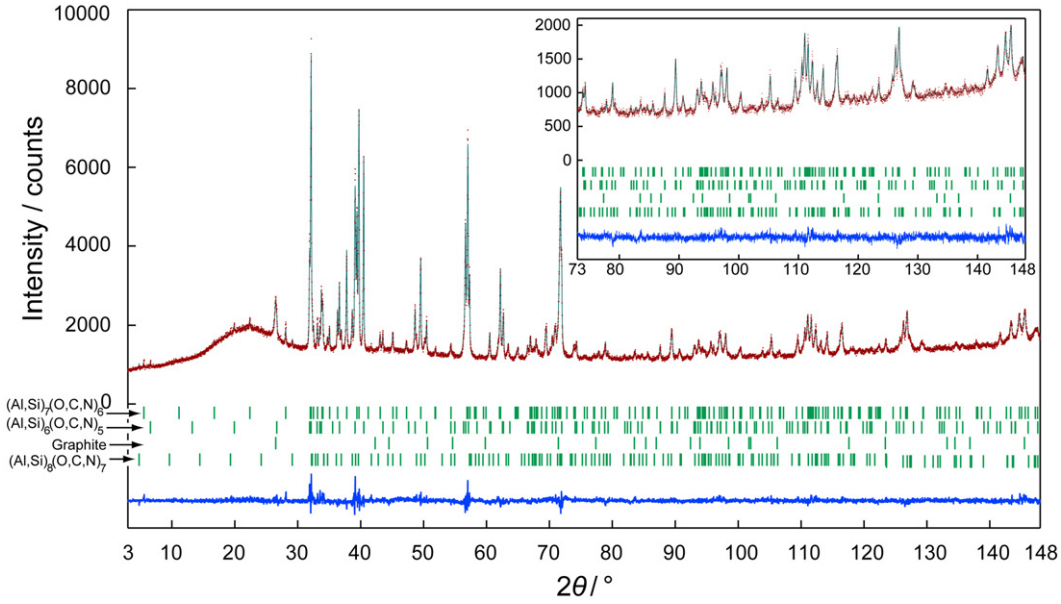

Fig. 7. Comparison of the observed diffraction pattern of $(Al_{5.8}Si_{1.2})(O_{1.0}C_{3.5}N_{1.5})$, $(Al, Si)_6(O, C, N)_5$, graphite and $(Al_{6.6}Si_{1.4})(O_{0.7}C_{4.3}N_{2.0})$ (symbol: +) with the corresponding calculated pattern (upper solid line). The difference curve is shown in the lower part of the diagram. Vertical bars indicate the positions of Bragg reflections.

Table 1
Crystal data for $(Al_{5.8}Si_{1.2})(O_{1.0}C_{3.5}N_{1.5})$.

Chemical composition	$Al_{5.82(6)}Si_{1.18(6)}O_{1.04(6)}C_{3.5(3)}N_{1.50(9)}$
Space group	$P6_3/mmc$
a (nm)	0.322508(4)
c (nm)	3.17193(4)
V (nm^3)	0.285717(6)
Z	2
D_x (Mgm^{-3})	3.13

Table 2
Structural parameters for $(Al_{5.8}Si_{1.2})(O_{1.0}C_{3.5}N_{1.5})$.

Site	Wyckoff position	g	x	y	z	$100 \times B$ (nm^2)
Al/Si1	4*e*	1	0	0	0.10847(6)	0.81(4)
Al/Si2	4*e*	1/2	0	0	0.2398(1)	1.01(9)
Al/Si3	4*f*	1	1/3	2/3	0.03142(6)	1.22(5)
Al/Si4A	4*f*	0.746(8)	1/3	2/3	0.1843(1)	1.16(7)
Al/Si4B	4*f*	0.254	1/3	2/3	0.1651(4)	1.16
O/C/N1	2*a*	1	0	0	0	1.06(5)
O/C/N2	2*c*	1	1/3	2/3	1/4	1.06
O/C/N3	4*e*	1	0	0	0.1700(2)	1.06
O/C/N4	4*f*	1	1/3	2/3	0.0917(2)	1.06

Table 3
Crystal data for $(Al_{6.6}Si_{1.4})(O_{0.7}C_{4.3}N_{2.0})$.

Chemical composition	$Al_{6.6}Si_{1.4}O_{0.7}C_{4.3}N_{2.0}$
Space group	$R\bar{3}\,m$ or $R3m$
a (nm)	0.32114(2)
c (nm)	5.5097(3)
V (nm^3)	0.49208(4)
Z	3
D_x (Mgm^{-3})	3.12

3.4. Structure description

In previous studies, each of the crystals $(Al, Si)_{18}(O, C)_{14}$, $(Al, Si)_5(O, C)_4$, $Al_5(O, C, N)_4$ and $(Al, Si)_6(O, C)_5$ has been found to be made up of two or three domains, which are related by pseudo-symmetry inversion [6–9]. One of the most plausible explanations to interpret the disordered crystal structure of $(Al, Si)_7(O, C, N)_6$ is to, in a similar manner, consider the structure to be a statistical average of several structural configurations. We have successfully extracted four types of ordered structural models I, II, III and IV (Fig. 8) from the parent disordered structural model (Fig. 5). The models I, II and III are characterized by the absence of Al/Si4B site. On the other hand, Al/Si4B site is required for the model IV. The layer stacking sequences within the unit cells are ⟨*BBABBBAB*⟩ for model I, ⟨*BABBBABB*⟩ for model II, ⟨*ABBBABBB*⟩ for model III and ⟨*BBBABBBA*⟩ for model IV (Fig. 8). All these crystal structures are noncentrosymmetric with the space group $P6_3mc$. When the center of symmetry is removed from the space group $P6_3/mmc$, the resulting space group is $P6_3mc$. The two structural configurations of I and II and those of III and IV are therefore related by a pseudo-symmetry inversion. As a result, the crystal must be composed of four types of domains, two of which are related by inversion twinning. Because the site occupancies of the parent disordered model are 1/2 for Al/Si2, and nearly equal to 3/4 for Al/Si4A and 1/4 for Al/Si4B, the domain ratios should be almost 1/4:1/4:1/4:1/4.

In Table 4, only Al/Si–O/C/N bonds belonging to one of the four structural configurations are reported, excluding possible bonds between atoms of different orientation states. With structural models I, II and III, the Al/Si4B–O/C/N bonds are missing because of the absence of Al/Si4B site for these models. On the other hand, there are no Al/Si4A–O/C/N bonds for the structural model IV due to the lack of Al/Si4A site. All of the Al/Si atoms in these four types of models are tetrahedrally coordinated by O/C/N atoms with the mean Al/Si–O/C/N distances of 0.198 nm, which are comparable to the mean Al/Si–O/C/N distances of $[(Al, Si)(O, C, N)_4]$ polyhedra in $(Al, Si)_{18}(O, C)_{14}$ (0.205 nm), $(Al, Si)_5(O, C)_4$ (0.202 nm), $Al_5(O, C, N)_4$ (0.202 nm) and $(Al, Si)_6(O, C)_5$ (0.200 nm). There is a possibility of site preference of Al and Si in the Al/Si sites. Hence we tried to extract the information on site preference from the Al/Si–O/C/N distances; however the obtained results could not be regarded as significant. The mean interatomic distance as well as atomic configurations of the model I (Fig. 8a) compare well with those of $Al_7C_3N_3$ (Fig. 1a). Thus, $(Al, Si)_7(O, C, N)_6$ can be described as being homeotypic to $Al_7C_3N_3$. The general formula of the oxycarbonitride is expressed by $(Al_{7-x}Si_x)(O_yC_zN_{6-y-z})$, where x-, y- and z-values are, respectively, 1.2, 1.0 and 3.5 for the sample.

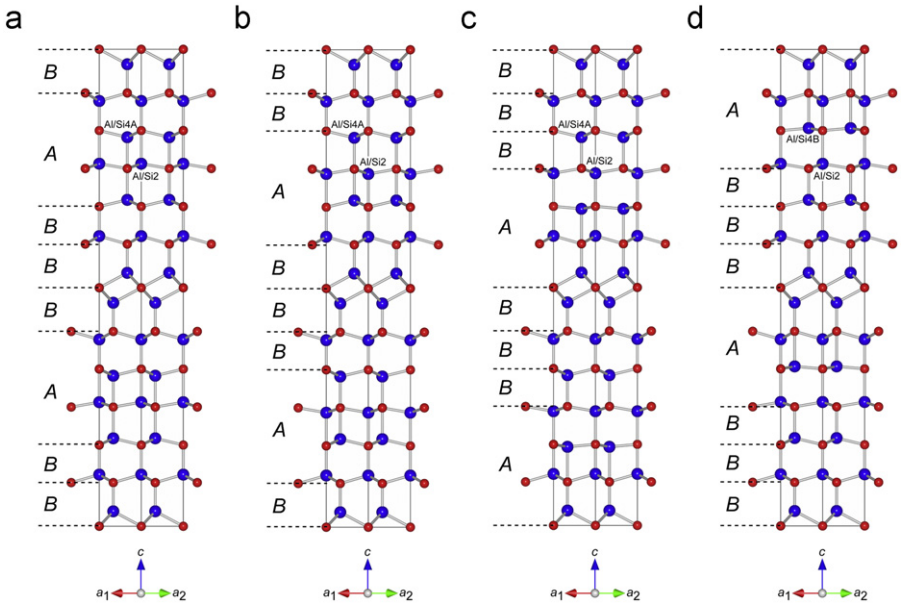

Fig. 8. Crystal structures of the four orientation states of $(Al_{5.8}Si_{1.2})(O_{1.0}C_{3.5}N_{1.5})$ viewed along [1 1 0], showing the crystal structures being made up of two types of layers *A* and *B*. Space group $P6_3mc$. The two structural configurations (a) and (b), and those of (c) and (d) are related by the pseudo-symmetry inversion.

Table 4
Interatomic distances (nm) in $(Al_{5.8}Si_{1.2})(O_{1.0}C_{3.5}N_{1.5})$.

Al/Si1–O/C/N4	0.19363(15) × 3
Al/Si1–O/C/N3	0.1953(6)
〈Al/Si1–O/C/N〉	0.1940
Al/Si2–O/C/N2	0.18900(5) × 3
Al/Si2–O/C/N3	0.2212(6)
〈Al/Si2–O/C/N〉	0.1971
Al/Si3–O/C/N4	0.1913(5)
Al/Si3–O/C/N1	0.21119(9) × 3
〈Al/Si3–O/C/N〉	0.2062
Al/Si4A–O/C/N3	0.1916(2) × 3
Al/Si4A–O/C/N2	0.2085(4)
〈Al/Si4A–O/C/N〉	0.1958
Al/Si4B–O/C/N2	0.18686(11) × 3
Al/Si4B–O/C/N4	0.2328(13)
〈Al/Si4B–O/C/N〉	0.1983

3.5. Oxidation and nitridation reactions

Inside the electric furnace, a small amount of air that was adsorbed on the graphite insulation board would be continuously released during the heating process. Thus, the experimental oxygen partial pressure (P_{O_2}) of the sample was most probably kept near the carbon–carbon monoxide (CCO) buffer [8,9]. Based on the CCO buffer, the P_{O_2}-values are estimated to be 2.7×10^{-15} atm ($\log P_{O_2}=-14.57$) at 2073 K and 2.8×10^{-14} atm ($\log P_{O_2}=-13.56$) at 2273 K, in which the CO gas reacts with Al_4C_3 compound to form Al_2O_3 and graphite as follows (Fig. 9a):

$$Al_4C_3\ (s)+6CO\ (g)\rightarrow 2Al_2O_3\ (s)+9C\ (s).$$

On the other hand, the compound SiC is stable at temperatures between 2073 and 2273 K near the CCO buffer (Fig. 9b). Accordingly, for the synthesis of $(Al, Si)_5(O, C)_4$ at 2073 K using the carbide chemicals of Al_4C_3 and SiC, the oxidation reaction would occur only for the former carbide [8,9]. During further heating at 2273 K, the oxygen atoms would be continuously introduced into the aluminum silicon oxycarbides by the preferential oxidation of the Al_4C_3 component.

In a previous study, the authors have reveled the conversion mechanism from $(Al_{4.4}Si_{0.6})(O_{1.0}C_{3.0})$ to $(Al, Si)_6(O, C, N)_5$ during the heating process at 2273 K for 1 h, the chemical composition of the latter was determined to be $(Al_{5.2}Si_{0.8})(O_{1.6}C_{3.4})$ [8]. This conversion reaction, which is characterized by the increase in O/(O+C) ratio from 0.25 to 0.32 as well as the simultaneous formation of graphite, is most probably induced by the preferential oxidation of Al_4C_3 component in $(Al, Si)_5(O, C)_4$. On further heating for 2 h in the present study, the conversion reaction from $(Al, Si)_6(O, C)_5$ to $(Al, Si)_7(O, C, N)_6$ occurred, which is characterized by the decrease in C/(O+C+N) ratio from 0.75 to 0.58 and the incorporation of N atoms into the anion sites. This implies that not only the thermal oxidation of Al_4C_3 component in $(Al, Si)_6(O, C)_5$ but also the thermal nitridation of Al_2O_3 component proceeded. Actually, the compound Al_2O_3 is, although stable at 2073 K with $P_{N_2}<0.18$ atm, unstable at 2273 K with $P_{N_2}>0.03$ atm near the CCO buffer (Fig. 9a). It reacts with N_2 gas and graphite to form AlN and CO gas as follows:

$$Al_2O_3\ (s)+N_2\ (g)+3C\ (s)\rightarrow 2AlN\ (s)+3CO\ (g).$$

While the thermodynamic behaviors of Al_4C_3 and Al_2O_3 components in the crystal structures of aluminum silicon oxycarbonitrides might be different from those of the individual compounds Al_4C_3 and Al_2O_3, the oxidation and nitridation reactions would successively occur for the Al_4C_3 component during heating at 2273 K. The nitridation reaction was negligible at 2073 K, however significantly proceeded at 2273 K, indicating that the P_{N_2}-value of the gas phase in the furnace must be 0.03 atm $<P_{N_2}<$ 0.18 atm (Fig. 9a). Accordingly, the content of air (80 vol% N_2 and 20 vol% O_2) in the furnace atmosphere must have been at least 3.8 ($=100\times0.03/0.8$) vol%.

In the system Al–Si–O–C–N, the authors discovered and structurally characterized three types of new oxycarbonitrides, $(Al, Si)_7(O, C, N)_6$, $(Al, Si)_8(O, C, N)_7$ and $Al_5(O, C, N)_4$ [9], and three types of new oxycarbides, $(Al_{16.8}Si_{1.2})(O_{3.0}C_{11.0})$ [6], $(Al, Si)_5(O, C)_4$ [7] and $(Al, Si)_6(O, C)_5$ [8]. These materials have the characteristics of the layered structures, hence the general formula is expressed by

$$(Al, Si)_{4l+m}(O, C, N)_{3l+m}$$

where *l* and *m* are, respectively, the numbers of *A*-type $[(Al, Si)_4(O, C, N)_4]$ unit layer and *B*-type $[(Al, Si)(O, C, N)_2]$ single layer of

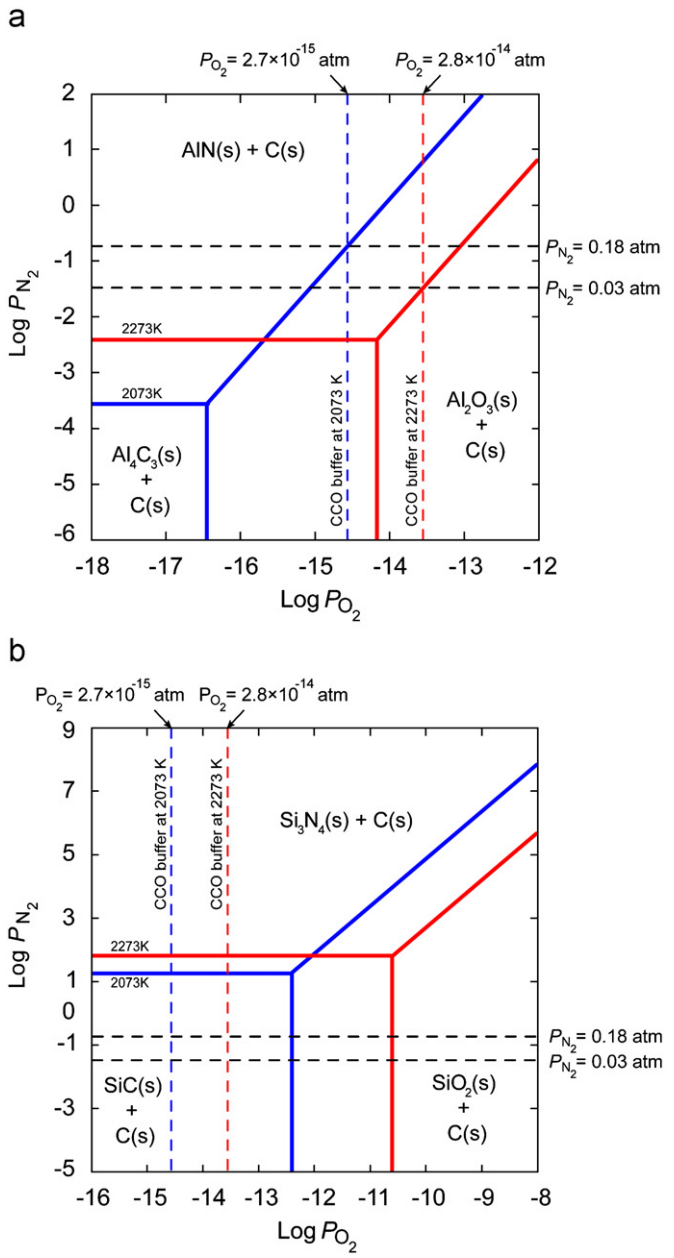

Fig. 9. Phase boundaries in the systems (a) Al–O–C–N and (b) Si–O–C–N as functions of oxygen partial pressure and nitrogen partial pressure. The phase boundaries, which are depicted by blue solid lines for 2073 K and red solid lines for 2273 K, are calculated using data from [21]. The broken lines of carbon–carbon monoxide (CCO) buffer at 2073 and 2273 K are from [22] (For interpretation of the references to color in this figure legend, the reader is referred to the web version of this article.)

the minimum stacking sequence. The (l, m) values are (2, 1) for $(Al, Si)_{18}(O, C)_{14}$, (1, 1) for $(Al, Si)_5(O, C)_4$, $Al_5(O, C, N)_4$, (1, 2) for $(Al, Si)_6(O, C)_5$, (1, 3) for $(Al, Si)_7(O, C, N)_6$ and (1, 4) for $(Al, Si)_8(O, C, N)_7$. Further work is necessary to confirm the existence of the other new aluminum silicon oxycarbonitrides having the (l, m) values with $(1, \geq 5)$, $(2, \geq 2)$ and/or $(\geq 3, \geq 1)$.

4. Conclusion

In the Al–Si–O–C–N system, we have successfully synthesized a new $Al_7C_3N_3$-homeotypic aluminum silicon oxycarbonitride, $(Al_{7-x}Si_x)$ $(O_yC_zN_{6-y-z})$ ($x\sim1.2$, $y\sim1.0$ and $z\sim3.5$). The crystal structure was satisfactorily represented by the split-atom model with the space group $P6_3/mmc$ (centrosymmetric). The crystal was composed of four types of domains with an almost 1/4:1/4:1/4:1/4 domain ratio. The dimension of twin domains was within the coherence range of X-rays, hence the crystal structure was successfully represented by the split-atom model. The new compound was most probably formed by the preferential oxidation of Al_4C_3 component in $(Al_{5.2}Si_{0.8})(O_{1.6}C_{3.4})$ and subsequent nitridation of the resulting Al_2O_3 component. The existence of another new aluminum silicon oxycarbonitride $(Al_{6.6}Si_{1.4})(O_{0.7}C_{4.3}N_{2.0})$ has been also demonstrated.

Acknowledgment

Supported by a Grant-in-Aid for Scientific Research (No. 21360322) from the Japan Society for the Promotion of Science.

Appendix A. supplementary Materials

Supplementary data associated with this article can be found in the online version at doi:10.1016/j.jssc.2011.06.030.

References

[1] Y.-C. Wu, T.-M. Chen, C.-H. Chiu, C.-N. Mo, J. Electrochem. Soc. 157 (2010) J342–J346.
[2] V.A. Zhilyaev, Yu.G. Zainulin, S.I. Alyamovskii, G.P. Shveikin, Powder Metall. Met. Ceram. 11 (1972) 632–636.
[3] M.R. Mucalo, N.B. Milestone, I.W.M. Brown, J. Mater. Sci. 32 (1997) 2433–2444.
[4] G.A. Jefeerey, V.Y. Wu, Acta Crystallogr. 16 (1963) 559–566.
[5] G.A. Jefeerey, V.Y. Wu, Acta Crystallogr. 20 (1966) 538–547.
[6] T. Iwata, M. Kaga, H. Nakano, K. Fukuda, J. Solid State Chem. 182 (2009) 2252–2260.
[7] M. Kaga, T. Iwata, H. Nakano, K. Fukuda, J. Solid State Chem. 183 (2010) 636–642.
[8] M. Kaga, D. Urushihara, T. Iwata, K. Sugiura, H. Nakano, K. Fukuda, J. Solid State Chem. 183 (2010) 2183–2189.
[9] H. Inuzuka, M. Kaga, D. Urushihara, H. Nakano, T. Asaka, K. Fukuda, J. Solid State Chem. 183 (2010) 2570–2575.
[10] E. Parthé, L.M. Gelato, Acta Crystallogr. A40 (1984) 169–183.
[11] L.M. Gelato, E. Parthé, J. Appl. Crystallogr. 20 (1987) 139–143.
[12] F. Izumi, K. Momma, Solid State Phenom. 130 (2007) 15–20.
[13] K. Momma, F. Izumi, J. Appl., Crystallogr. 41 (2008) 653–658.
[14] A. Le Bail, H. Duroy, J.L. Fourquet, Mater. Res. Bull. 23 (1988) 447–452.
[15] A. Altomare, M.C. Burla, M. Camalli, B. Carrozzini, G.L. Cascarano, C. Giacovazzo, A. Guagliardi, A.G.G. Moliterni, G. Polidori, R. Rizzi, J. Appl. Crystallogr. 32 (1999) 339–340.
[16] H.M. Rietveld, J. Appl. Crystallogr. 2 (1969) 65–71.
[17] H. Toraya, J. Appl. Crystallogr. 23 (1990) 485–491.
[18] W.A. Dollase, J. Appl. Crystallogr. 19 (1986) 267–272.
[19] R.A. Young, in: R.A. Young (Ed.), The Rietveld Method, Oxford University Press, Oxford, U.K, 1993, pp. 1–38.
[20] G.W. Brindley, Bulletin de la Societe Chimique de France (1949) D59–63.
[21] M.W. Chase Jr. (Ed.), NIST-JANAF Thermochemical Tables, J. Phys. Chem. Ref. Data Monograph No. 9, 4th ed.,American Chemical Society and American Institute of Physics, Woodbury, NY, 1998.
[22] I.S. Kulikov, Thermodynamics of Oxides, Metallurgiya, , 1986.